Received: 12 January 2024 | Revised: 29 March 2024 | Accepted: 22 May 2024

DOI: 10.1002/jemt.24624

RESEARCH ARTICLE

MICROSCOPY RESEARCH & TECHNIQUE WILEY

Comparative macroanatomical and scanning electron microscopy study of the eyeball in brachycephalic and mesocephalic dog breeds

Cengizhan Yılmaz[1] | Murat Kabak[2] | Sedef Selviler Sizer[2]

[1]Graduate School of Educational Sciences, Ondokuz Mayis University, Samsun, Turkey

[2]Faculty of Veterinary Medicine, Department of Anatomy, Ondokuz Mayis University, Samsun, Turkey

Correspondence
Sedef Selviler Sizer, Faculty of Veterinary Medicine, Department of Anatomy, Ondokuz Mayis University, Samsun 55200, Turkey.
Email: sedef.selviler@omu.edu.tr

Review Editor: Paul Verkade

Abstract

The anatomical structures forming the eyeball differ among dog breeds, both morphologically and morphometrically. This study was aimed at determining the morphometric values of the eyeball layers of different dog breeds and the morphological structures of these layers using scanning electron microscopy. Thirty-two eyeballs of 17 dogs belonging to 9 different breeds that died from traffic accidents, falling from a height, and naturally were used. These dog breeds were grouped according to their brachycephalic and mesocephalic skull structures, and morphometric measurements of the eyeballs of each group were obtained. Scanning electron microscopy was used to examine the morphological structure of the eyeball layers. The studied dogs' eyeballs comprised three layers: outer, middle, and inner. Thickness measurements obtained from three different regions of the eyeball indicated that the equatorial region was the thinnest among all dog breeds. Moreover, the cornea, which is covered by the sclera along its edges, was thicker at the corneal limbus than at the corneal vertex. A positive correlation was observed between lens thickness and the number of ciliary processes, which varied according to the dogs' head structures. Notably, depression was observed in the posterior surface of the lens in brachycephalic dogs. The morphometric values of the eyeball layers in the brachycephalic and mesocephalic dog breeds were also determined. These values will help researchers study this subject, and the determined morphometric and morphological values will contribute to the anatomy literature.

Research Highlights

- This comprehensive study investigates the morphometric and morphological variations in the eyeball layers of different dog breeds, utilizing scanning electron microscopy to analyze eyeballs. It reveals significant breed-specific differences,

This study is part of a master's thesis.

This is an open access article under the terms of the Creative Commons Attribution-NonCommercial-NoDerivs License, which permits use and distribution in any medium, provided the original work is properly cited, the use is non-commercial and no modifications or adaptations are made.
© 2024 The Author(s). *Microscopy Research and Technique* published by Wiley Periodicals LLC.

particularly between brachycephalic and mesocephalic dogs, regarding eyeball layer thickness, corneal structure, lens thickness, and the number of ciliary processes.

KEYWORDS
anatomy, dog breeds, eyeball, morphometric values, scanning electron microscopy

1 | INTRODUCTION

An eyeball comprises three layers: the outer, middle, and inner (Murphy et al., 2013). The outer layer is fibrous, consisting of hard connective tissue, and less vascularized; it has two components: the sclera and cornea (Dyce et al., 2009; König & Liebich, 2020). The cornea consists of five layers: the epithelium, Bowman's layer, stroma, Descemet's membrane, and endothelium (König & Liebich, 2020; Leeson et al., 1985; Murphy et al., 2013). The middle layer is a thick layer that is located between the retina and sclera and contains the choroid, ciliary body, and iris (König & Liebich, 2020; Leeson et al., 1985; Murphy et al., 2013). The choroid is the pigmented vascular layer of the eyeball. (Akers & Denbow, 2013; Leeson et al., 1985). The ciliary body, which is continuous with the choroid, circularly thickens around the lens and includes wraps called ciliary plicae. Combining a few of these wraps creates major and minor processes. The number of ciliary processes in dogs varies between 50 and 90 pieces (Diesem, 1975; Tanimura, 1977). The outermost fibers of the ciliary muscle, located between the ciliary processes and the sclera on the outer surface of the ciliary body, are longitudinal meridional fibers (Brücke's muscle). The innermost circular or radial muscle fibers are circular fibers (Müller muscle). The inner layer—the retina, which exists as a thin membrane—is the innermost layer of the eyeball (Bacha et al., 2012; Murphy et al., 2013). The average thickness of the retinal nerve fiber layer in dogs is 141.69 (±18) μm, and the fiber thicknesses in the anterior and posterior regions vary [148.03 (±8.5) μm and 141.06 (±8.73) μm, respectively] (García-Sánchez et al., 2007). The lens is a soft, transparent, and protein-rich biconvex structure suspended between the posterior surface of the iris and the anterior surface of the vitreous body. The dorsoventral length of the lens in dogs is 9–10 mm, whereas the anterior–posterior length is 7 mm (Diesem, 1975; Leeson et al., 1985). The eyeball diameter of dogs is reportedly 20 (±1.6) mm, the axial lens thickness is 6.7 (±1.0) mm, and the axial lens thickness/sphere diameter ratio is 0.33 (±0.1). Morphological examination of the lens was conducted using ultrasonography (Chiwitt et al., 2017; Diesem, 1975; König & Liebich, 2020; Murphy et al., 2013). Some studies have assessed the morphometric values and morphological structure of the eyeballs of horses, cattle (Patruno et al., 2017), goats (Kassab & El-Zoghby, 2010), and pigs (Mc Menamin & Steptoe, 1991; Patruno et al., 2017). Relative to the animal's body size, cats, followed by dogs, horses, cattle, and pigs, have the largest eyeball (König & Liebich, 2020). A study conducted in dogs reported that the radius of the eyeball varies according to breed (range, 9.56–11.57 mm), and that this measurement is proportional to the length and width of the skull (McGreevy et al., 2003). By contrast, Chiwitt et al. (2017) reported that the eyeball size varies with the animal's weight and not its head structure and sex. The eye positions, orbital sizes, and palpebral aperture sizes and shapes vary considerably across different dog breeds (Murphy et al., 2013). Various studies have been conducted to assess the morphometric values of the eyeballs of dogs categorized according to breed (Gaiddon et al., 1991; Gilger et al., 2005; Gwin et al., 1982; Kreuzer & Sivak, 1985; Murphy et al., 1992; Mutti et al., 1999; Schiffer et al., 1982) and head structure (Chiwitt et al., 2017). However, comparatively detailed morphometric values of the eyeball have not yet been reported for dog breeds with brachycephalic and mesocephalic head structures. Additionally, no information is available regarding the scanning electron microscopic structures for some dog breeds assessed in our study (Kangal, Pomeranian, German Shepherd, and Pug breeds).

2 | MATERIALS AND METHODS

2.1 | Animal materials

Different dog breeds that died due to traffic accidents, falling from height, and natural death were used in the study. These dog breeds were grouped according to brachycephalic (six dogs) and mesocephalic (three dogs) head structures. In post-mortem examinations, eyeballs without anatomical deformation were detected with 10% formaldehyde. Thirty-two eyeballs from 17 dogs from 9 different breeds were examined.

2.2 | Anatomical examination

The cornea was separated by dissection at the corneal limbus level for morphometric measurements of the iris and pupil. The thickness of the eyeball was measured at the level of the ciliary body, equator, and optic nerve. All morphometric measurements were taken with a digital caliper (Mitutoyo, Japan). Parts of the eyeball, such as the iridocorneal angle and ciliary body, were examined through dissections performed under a stereomicroscope (Olympus SZ61 TRC) and photographs were taken with an Olympus brand (Olympus C-5060) camera.

2.3 | Examination in scanning electron microscopy

To examine under scanning electron microscopy, samples from the cornea, lens, iris, choroid and ciliary body of mesocephalic (German shepherd and kangal) and brachycephalic (pug and Miniature Pinscher) dogs were fixed in 2.5% glutaraldehyde solution and then washed with phosphate buffer solution (PBS). Then, the tissues were treated with 1% osmium tetroxide. Afterward, the samples were dehydrated with serial acetone dilutions, dried with Quorum K850 (Critical Point Dryer) and coated with gold–palladium (Au/Pd). Then, the samples of the eyeballs were examined under a scanning electron microscope (JEOL, JSM-7001F) and images were obtained at different magnifications.

2.4 | Statistical analysis

For the main groups, subgroupings were made based on sex (male and female) and eye direction (right eye and left eye), and the examined features were summarized based on this grouping. The data were summarized by calculating the arithmetic mean and standard errors of the means from descriptive statistics. Differences in the examined characteristics according to groups were arranged according to random parcels and evaluated in a factorial trial design. Differences in the examined characteristics according to groups were arranged according to random parcels and evaluated in a factorial trial design. ANOVA analysis technique was used for statistical evaluations between subgroups with simple effects between the main group (brachycephalic and mesocephalic) subgroup averages. The DUNCAN test, one of the multiple comparison tests, was used to determine the differences between the group averages, and the TUKEY multiple comparison test was used to compare the interaction effects between the groups. In the study, the dorsoventral and lateromedial lengths of the lens and the lens thickness were also measured from lens measurements, and the Spearman rank correlation was calculated and interpreted to reveal the correlations between lens thickness and ciliary process numbers (Easterling, 2015). All calculations regarding the data used in the study were made in the statistical package program (SAS: SAS Statistic software ver. 9.3.1, 2009).

3 | RESULTS

The eyeball morphometric measurements for all the dog breeds assessed in the present study are shown in Table 1. For all breeds, the external axis of the eyeball length was observed to be smaller than that of the equatorial length (Figure 1a). The thinnest part of the eyeball was found to be at the equatorial line in all the examined dogs. The eyeball morphometric values did not vary according to breed, sex, age, or weight in the mesocephalic and brachycephalic dogs. The results of the statistical analyses for the mesocephalic and brachycephalic breeds are summarized in Table 2. Morphometrically, the differences between the brachycephalic and mesocephalic dogs were significant ($p < .01$) when the classification results of the equatorial length and external axis of eyeball characteristics according to head size were evaluated. For the same parameters, intra-group and inter-group differences according to sex and the direction of the measured organ were found to be non-significant ($p > .05$). Differences in the

TABLE 1 Mean morphometric values (mm) of the eyeball in different dog breeds.

	German Shepherd	Kangal	Golden	Rottweiler	Husky	Dogo	Pug	Pomeranian	Miniature Pinscher
Equatoral length	23.84	27.48	23.59	25.96	23.53	23.26	17.86	16.00	16.90
External axis of the eyeball length	21.28	24.52	22.32	23.95	21.76	20.95	16.64	13.84	14.91
Equatorial thickness of the Eyeball	0.66	0.69	0.68	0.72	0.71	0.64	0.56	0.50	0.54
Thickness of eyeball at the level of the ciliary body	1.45	1.68	1.38	1.60	1.41	1.59	1.03	0.90	0.91
Thickness of eyeball at the level of optic nerve	1.54	1.69	1.48	1.69	1.52	1.62	1.11	0.79	0.87
Thickness of the corneal vertex	0.66	0.69	0.63	0.64	0.64	0.70	0.55	0.53	0.53
Thickness of the corneal limbus	0.70	0.74	0.68	0.70	0.68	0.72	0.59	0.57	0.59
Dorsal width of the iris	4.15	5.40	4.20	4.98	3.41	4.48	3.20	2.40	2.31
Ventral width of the iris	4.08	5.53	4.21	4.70	3.37	4.53	3.15	2.47	2.34
Median width of the iris	4.12	5.44	4.24	5.02	3.39	4.54	3.17	2.38	2.28
Lateral width of the iris	4.30	5.66	4.36	5.28	3.86	4.85	3.62	2.77	2.75
Dorsoventral opening of the pupil	8.32	9.56	8.06	9.16	7.73	9.11	6.38	5.28	5.11
Lateromedial opening of the pupil	8.73	9.87	8.46	9.47	7.97	9.38	7.17	5.66	5.61
Equator lentis length	12.31	13.04	12.04	12.74	11.88	12.08	7.78	6.82	6.41
Axis lentis length	11.05	12.88	11.44	11.69	10.24	11.22	7.50	5.57	6.15
Lens thickness	7.80	8.14	6.90	7.92	6.64	8.06	5.07	4.90	5.02

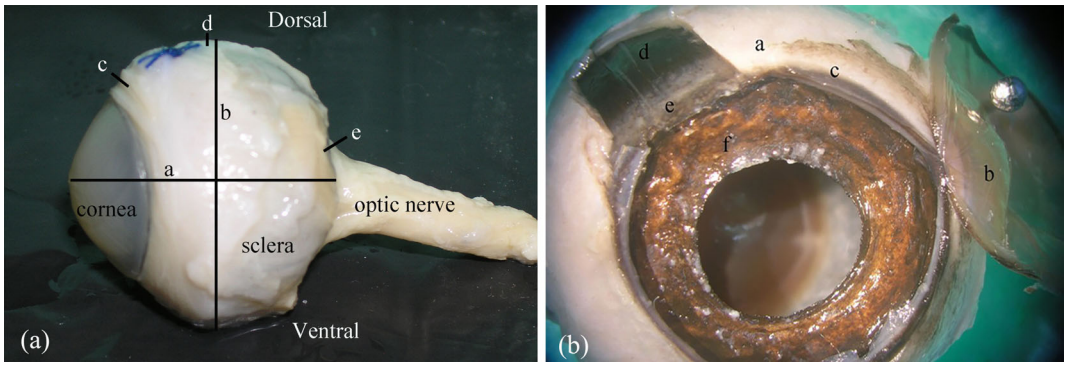


FIGURE 1 (a) General view of the eyeball. a: external axis of the eyeball, b: equator, c: measurement site at the level of the ciliary body, d: measurement site at the level of the equator, and e: measurement site at the level of the optic disc. (b) View of the anatomical structures of the eyeball of a German shepherd dog. a: sclera, b: cornea, c: corneal limb, d: choroidea, e: ciliary body and f: iris.

TABLE 2 Statistical values regarding morphometric values (mm) of Eyeball.

	General		Brachycephalic		Mesocephalic	
Features	***N***	$\overline{X} \pm S_{\overline{X}}$	***N***	$\overline{X} \pm S_{\overline{X}}$	***N***	$\overline{X} \pm S_{\overline{X}}$
Equatorial length	32	21.44 ± 0.75	13	16.70 ± 0.21b	19	24.68 ± 0.44a
Axis of the eyeball length	32	19.34 ± 0.73	13	14.76 ± 0.28b	19	22.47 ± 0.40a
Thickness of eyeball at equatorial level	32	0.62 ± 0.01	13	0.52 ± 0.01b	19	0.68 ± 0.01a
The thickness of the eyeball at the level of the ciliary body	32	1.27 ± 0.05	13	0.92 ± 0.01b	19	1.51 ± 0.03a
Thickness of eyeball at the level of optic disc	32	1.29 ± 0.06	13	0.87 ± 0.03b	19	1.58 ± 0.02a
Corneal vertex thickness	32	0.61 ± 0.01	13	0.53 ± 0.01b	19	0.66 ± 0.01a
Corneal limbus thickness	32	0.65 ± 0.01	13	0.58 ± 0.01b	19	0.70 ± 0.01a
Dorso-ventral opening of the pupil	32	7.30 ± 0.30	13	5.37 ± 0.13b	19	8.62 ± 0.14a
Latero-medial opening of the pupil	32	7.71 ± 0.29	13	5.87 ± 0.16b	19	8.96 ± 0.14a
The medial width of the iris	32	4.03 ± 0.20	13	2.83 ± 0.15b	19	4.85 ± 0.12a
The lateral width of the iris	32	3.99 ± 0.18	13	2.88 ± 0.09b	19	4.74 ± 0.13a
The dorsal width of the iris	32	3.66 ± 0.19	13	2.48 ± 0.09b	19	4.47 ± 0.14a
The ventral width of the iris	32	3.65 ± 0.18	13	2.53 ± 0.08b	19	4.42 ± 0.14a

Note: a,b, Differences between group means with different letters in the same rows are significant at $p < .01$ level.
Abbreviations: $S_{\overline{X}}$, standard deviation of the mean; $\overline{X}$, arithmetic mean.

eyeball thickness measurement values based on brachycephalic and mesocephalic head structures were significant (P < 0.01). The eyeball was found to comprise three layers in all of the examined dog breeds: the outer, middle, and inner layers.

The outer layer consisted of the sclera and cornea (Figure 1); the cornea was covered by the sclera along its edges. The thickness of the corneal limbus was greater than that of the corneal vertex in all breeds (Table 1). In dogs with a mesocephalic skull structure, the average corneal limbus thickness was 0.70 ± 0.01 mm, whereas the average corneal vertex thickness was 0.66 ± 0.01 mm. In dogs with a brachycephalic head structure, the corneal limbus thickness was 0.58 ± 0.01 mm, whereas the corneal vertex thickness was 0.53 ± 0.01 mm. The optic disc, the point at which the optic nerve enters the eyeball in the posterior part of the sclera, was quite prominent in all breeds (Figure 2a). The cornea was determined to comprise four layers in all of the examined dog breeds because Bowman's layer, which is one of the layers forming the cornea, was not prominent (Figure 2b,c). The epithelium was quite prominent, and three rows of polygonal cells were present on the basal cells of this layer (Figure 2b). Collagen fibrils (Figures 2b,c) and corneal cells (Figure 2b,c) were observed in the corneal stroma. The endothelium was observed to consist of cubical, single-row epithelial cells (Figure 2d).

The middle layer of the eyeball was found to contain the choroid, ciliary body, and iris (Figure 3a). The choroid was observed to be pigmented and the largest region of the middle layer. The ciliary body comprised the orbiculus ciliaris (Figure 3a), ciliary corona (Figure 3a), and ciliary muscle. The orbiculus ciliaris is located between the choroid and ciliary corona and has a flat structure. The ciliary corona, which contains radial appendages, was found to contain ciliary plicae. The ciliary processes formed by the combination of ciliary plicae were of varying sizes (Figure 3b). The average number of ciliary processes

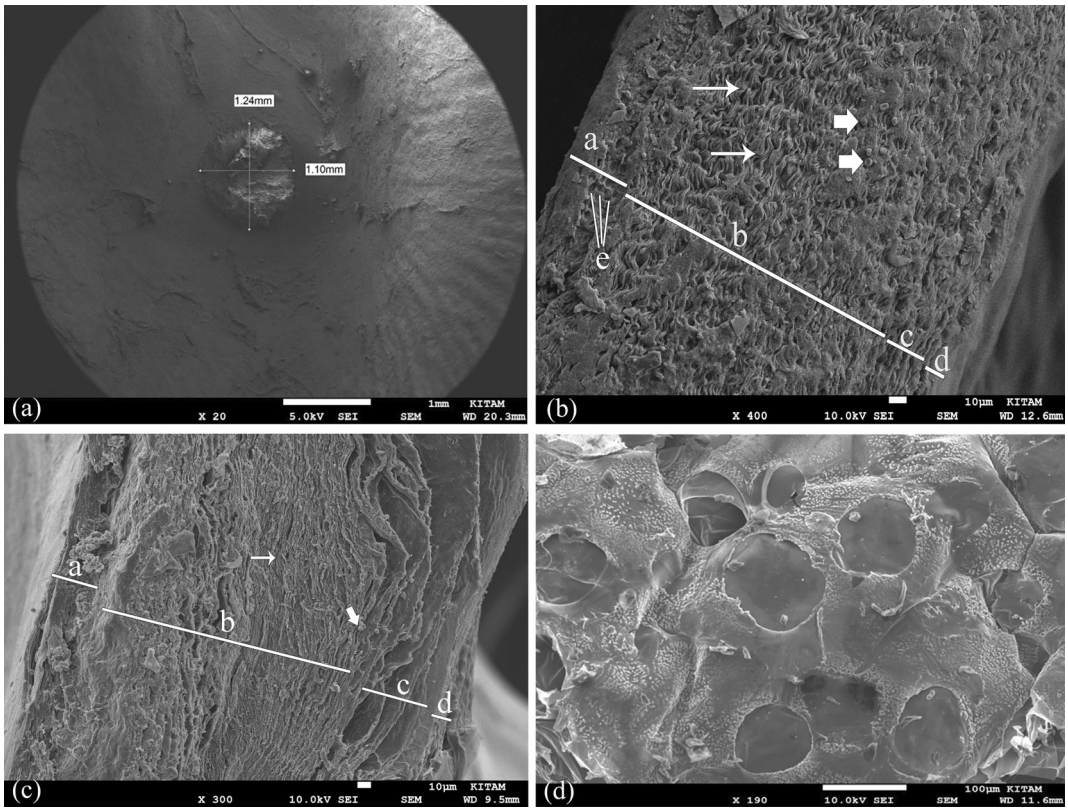


FIGURE 2 (a) SEM view of the optic disc in German shepherd dog, (b) SEM view of the cornea in Miniature Pincher. a: epithelium, b: stroma, c: Descemet's membrane, d: endothelium, e: polygonal cells thin arrow: collagen fibrils thick arrow: corneal cells, (c) SEM view of the cornea in a German shepherd dog. a: epithelium, b: stroma, c: Descemet's membrane, d: endothelium thin arrow: collagen fibrils thick arrow: corneal cells, and (d) SEM view of endothelium in German shepherd dog.

was 60 and 80 in dogs with brachycephalic and mesocephalic skull structures, respectively. In all dog breeds, zonular fibers, which are very thin and connected to the anterior and posterior ends of the lens, were detected starting from the tips of the ciliary processes (Figures 3 and 4a). The zonular fibers were present in the form of bundles in dogs with a brachycephalic head structure (Figure 4a) and as fibers in dogs with other head structures (Figure 3d). The anterior end of the ciliary process, where the zonular fibers start, was raised. Circular fibers, which are the innermost fibers of the ciliary muscles at the level of the beginning of the ciliary corona, were found to be circular (Figure 4b). An abundant reticular network existed between these circular muscle fibers and the minor and major ciliary processes (Figure 4c).

When the iris, which is the last part of the middle layer, was macroanatomically examined, the ciliary zone was found to be thicker than the pupillary zone. The depths of the iridial fold seen in the facies posterior and facies anterior of the iris were lesser, whereas the widths between the folds were greater (Figure 4d). The lateral, medial, dorsal, and ventral lengths of the iris were measured (Table 2). The lateral length was generally greater than that of the other parts in all the examined dog breeds. The pupil in the center of the iris was observed to be narrow and nearly round in all of the examined dog breeds. The lateromedial and dorsoventral apertures of the pupils are provided in Table 1. The lateromedial opening of the pupil was smaller than the dorsoventral opening in all of the examined dog breeds. In the iridocorneal angle, a trabecular meshwork and spaces of the iridocorneal angle were observed when the sclera and cornea were lifted upward with forceps (Figure 5a). The pectinate ligament starting from the iridocorneal angle and extending toward the iris was determined (Figure 5b). Because the inner layer (Figure 5c), which is the innermost layer of the eyeball, was very thinly formed, morphometric measurements of this layer could not be obtained.

The lens between the facies posterior of the iris and the vitreous body had a convex structure in all of the examined dog breeds. The posterior surface of the lens was hollow in the brachycephalic dogs (Figure 6a), whereas both sides of the lens were markedly convex in the mesocephalic dogs (Figure 6b). The equator lentis and axis lentis lengths of all of the examined dog breeds are presented in Table 1. Moreover, the statistical results pertaining to the equator lentis and axis lentis lengths, lens thickness, and the number of ciliary processes of dogs grouped according to the brachycephalic and mesocephalic head structures are shown in Table 3. Noteworthily, the morphometric values and number of ciliary processes were found to significantly differ according to the head structure ($p < .01$). When the sex and direction of the measured organs were evaluated within the groups, the differences were non-significant ($p > .05$). The relationship

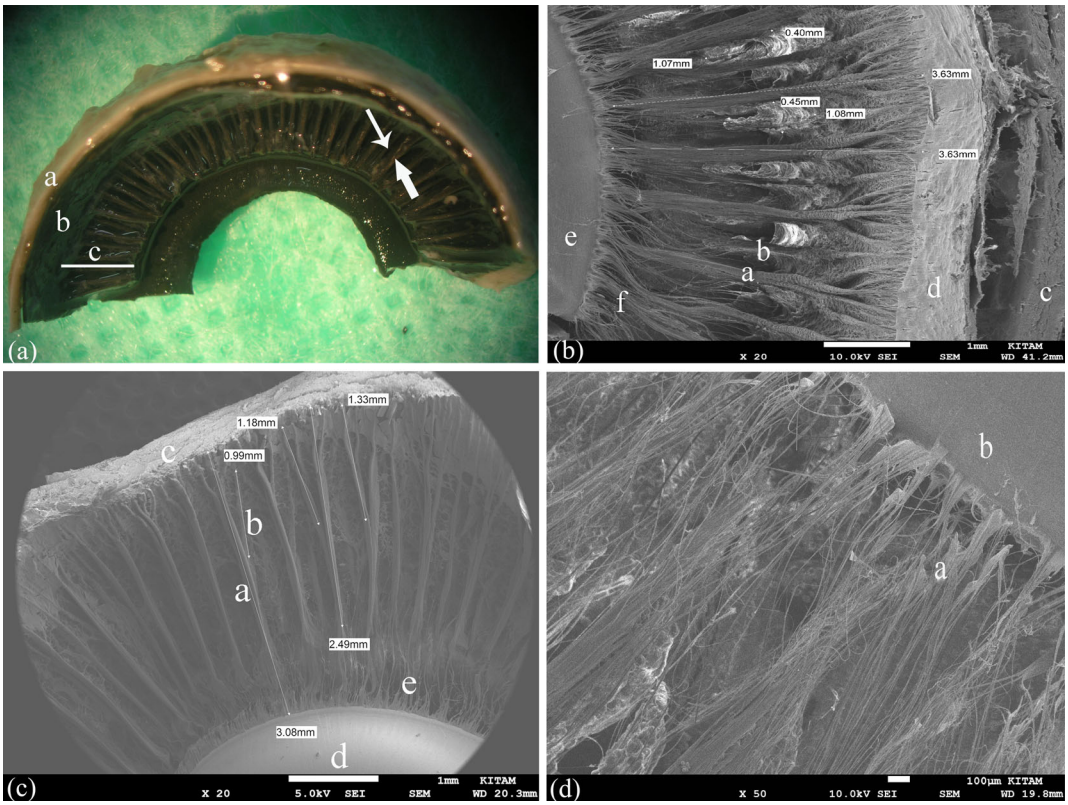


FIGURE 3 (a) Appearance of ciliary corona and processus ciliary in German Shepherd dog. a: sclera, b: orbiculus ciliaris, c: ciliary corona, thin arrow: minor ciliary processes, thick arrow: major ciliary processes, (b) SEM view of ciliary corona and ciliary processes lengths in German shepherd dog. a: major ciliary processes, b: minor ciliary processes, c: the sclera, d: orbiculus ciliaris, e: lens, and f: zonular fibers, (c) SEM view of the ciliary corona in the Pug dog. a: major ciliary processes, b: minor ciliary processes, c: orbiculus ciliaris, d: lens, and e: zonular fibers, and (d) SEM view of the attachment of the zonular fibers to the lens in a German shepherd dog. a: zonular fibers and b: lens.

between the equator lentis, axis lentis, lens thickness, and number of ciliary processes are shown in Table 4. Accordingly, in the general evaluation made without considering the groups, all of the investigated features had a strong positive correlation with the number of ciliary processes ($p < .01$). A significant positive correlation was noted between the lens thickness measurements and the number of ciliary processes in the mesocephalic dogs ($p < .05$). In the brachycephalic dogs, a negative correlation was found between the number of ciliary processes and both lens thickness and equatorial lentis length measurements, although the value was non-significant ($p > .05$). Moreover, a positive correlation was found between the axis lentis length measurements and the number of ciliary processes, although the value was non-significant ($p > .05$). The lens was found to contain a lens capsule on the outside and a lens cortex comprising intertwined layers under it (Figure 6c). Zonular fibers were found to adhere to the lens capsule. Variable hook-shaped structures were connected in the lens nucleus located at the center of the lens (Figure 6d).

4 | DISCUSSION

The dogs' eyeballs were found to contain three layers, and the anatomical structures that make up each layer were found to be generally consistent with those reported in the literature (König & Liebich, 2020). Morphometrically, many studies have measured and evaluated different areas of eyeballs. McGreevy et al. (2003) reported that the radius of dogs' eyeballs varies according to the skull structure and ranges between 9.56 and 11.57 mm. The same researchers also showed that the radius of the globe correlates with the length and width of the skull. In this study, we found that not only the diameter but also the external axis of the eyeball and the equatorial length vary with skull size.

The mean corneal limbus thickness and mean corneal vertex thickness were determined to be 0.70 ± 0.01 mm and 0.66 ± 0.01 mm in mesocephalic dogs and 0.58 ± 0.01 mm and 0.53 ± 0.01 mm in brachycephalic dogs, respectively. The mean corneal vertex thicknesses of 585 (±85) µm in one study (Kafarnik et al., 2007) and 611 µm in another study (Lynch & Brinkis, 2006) are consistent with those found in our study. Gaiddon et al. (1991) reported that the lateromedial length of the cornea is greater than the dorsoventral length, and that the lateromedial length of the cornea ranges between 16 and 18 mm for an average-sized dog. In the present study, we found that the lateromedial length of the cornea was 20 mm in large-breed dogs and 14 mm in small-breed dogs.

The cornea generally consists of five layers (Diesem, 1975; König & Liebich, 2020; Leeson et al., 1985; Murphy

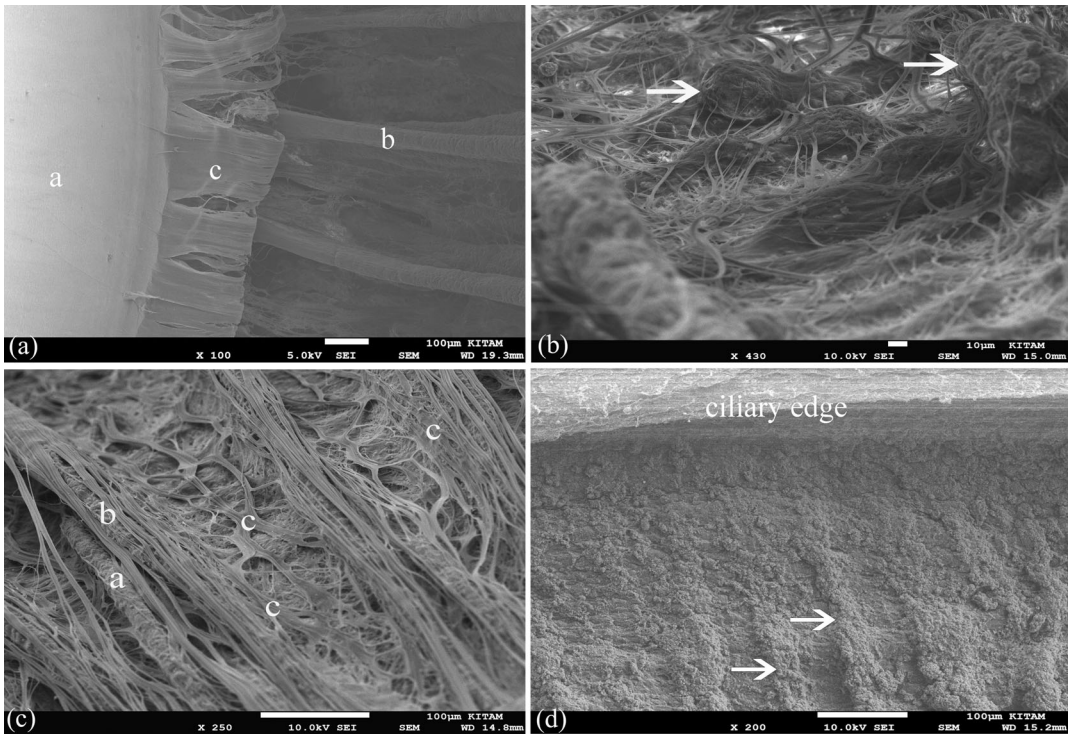


FIGURE 4 (a) SEM view of the zonular fibers in the pug dog. a: lens, b: major ciliary processes, and c: zonular fibers. (b) SEM view of ciliary muscle (arrows) in German shepherd dog, (c) SEM view of the reticular network structure in the ciliary corona. a: minor ciliary processes, b: major ciliary processes, and c: reticular meshwork, and (d) SEM view of the iridial fold (arrows) in the facies posterior of the iris.

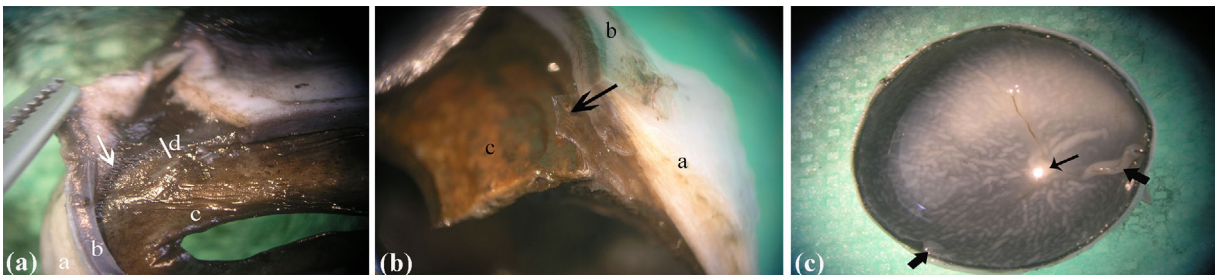


FIGURE 5 (a) Appearance of the iridocorneal angle in a Miniature Pincher, a: sclera, b: cornea, c: iris, and d: iridocorneal angle arrow: trabecular meshwork, (b) appearance of pectinate ligament in German shepherd dog. a: sclera, b: cornea, c: iris arow: pectinate ligament, and (c) internal view of the posterior part of the eyeball, thick arrows: retina, thin arrow: optic disc.

et al., 2013). Bowman's layer, which is modified from the stroma in dogs, is very thin (Getty, 1965) and cannot be determined (Bacha et al., 2012; Diesem, 1975; Murphy et al., 2013; Taşbaş, 1985). Murphy et al. (2013) reported that this layer was not visible in canine corneas and that it contained hypocellular and randomly distributed collagen bundles in the subepithelial stroma. In the present study, we analyzed the cornea as comprising four layers because Bowman's layer could not be determined. Three rows of polygonal cells have been found on the basal cells of the epithelium layer (Murphy et al., 2013), consistent with the findings of the present study.

The appearance of collagen fibrils and corneal cells in the corneal stroma is consistent with that reported in the literature (König & Liebich, 2020; Morishige et al., 2007). In the present study, the epithelium layers consisted of a single row of cubic cells, consistent with the reports of Bacha and Bacha et al. (2012) and Dyce et al. (2009). The literature contains different statements about the number of ciliary processes in the ciliary corona. Taşbaş (1985) reported that the number of ciliary processes was 50–70, König and Liebich (2020) and (Diesem, 1975) reported this number to be 70–80, and Murphy et al. (2013) reported approximately 76 pieces. In the present study, the average number of ciliary processes was found to be 60 in brachycephalic dog breeds and 80 in mesocephalic dog breeds. We determined that zonular fibers starting from ciliary processes existed in the form of bundles in brachycephalic dogs and as fibers in mesocephalic dogs. Our findings regarding mesocephalic dog breeds are consistent with

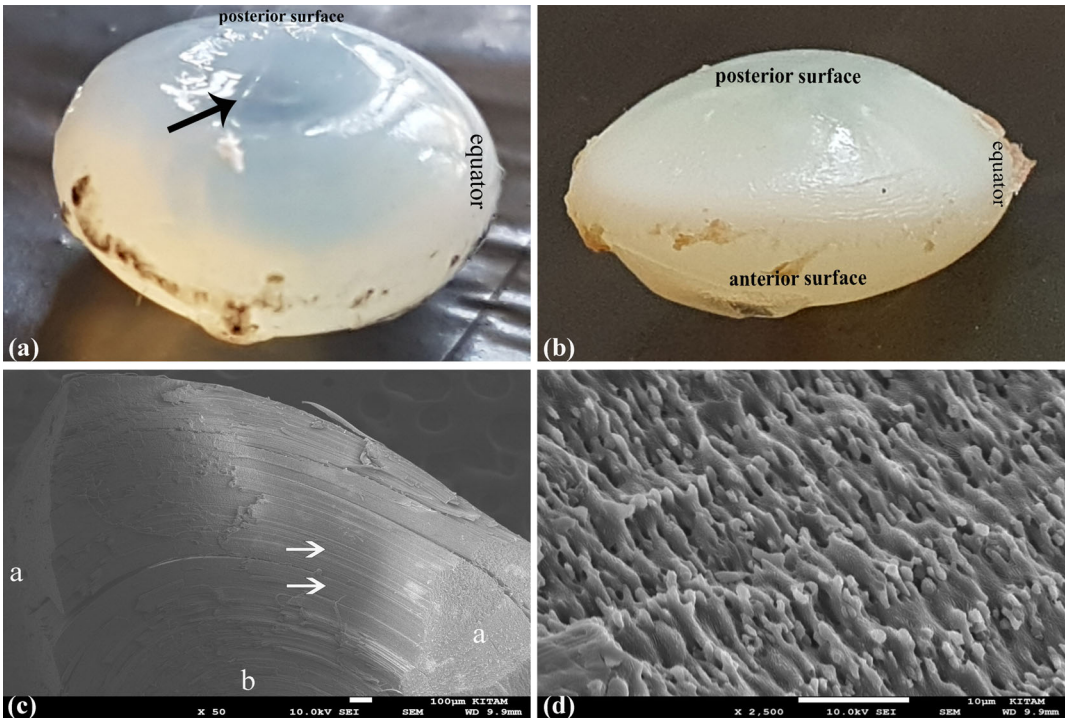


FIGURE 6 (a) Macroanatomical view of the lens in dogs with Brachycephalic skull structures, arrow: depression in facies posterior of the lens, (b) Macroanatomical view of the lens in dogs with mesocephalic skull structures. arrow: depression in facies posterior of the lens, (c) SEM view of the lens. a: lens capsule and b: lens nucleus arrows: laminae lentis, and (d) SEM view of hook-shaped structures in the lens nucleus.

TABLE 3 Morphometric values of the lens and statistical values (mm) of the number of ciliary processes.

	General		Brachycephalic		Mesocephalic	
Features	***N***	$\overline{X} \pm S_{\overline{X}}$	***N***	$\overline{X} \pm S_{\overline{X}}$	***N***	$\overline{X} \pm S_{\overline{X}}$
Equator lentis length	31	9.89 ± 0.55	12	6.08 ± 0.14b	19	12.29 ± 0.08a
Axis lentis length	31	9.43 ± 0.45	12	6.38 ± 0.12b	19	11.35 ± 0.15a
Lens thickness	31	6.58 ± 0.24	12	4.96 ± 0.02b	19	7.61 ± 0.13a
Number of ciliary processes	31	71.35 ± 2.06	12	59.00 ± 1.65b	19	79.15 ± 1.32a

Note: a,b: Differences between group means with different letters in the same rows are significant at $p < .01$ level.

TABLE 4 Spearman's rank correlation coefficients and correlation analysis results between the morphometric values (mm) of the lens and the number of ciliary processes.

	Number of ciliary processes		
Features	**General**	**Brachycephalic**	**Mesocephalic**
Equator lentis length	0.71 **	−0.26 NS	0.09 NS
Axis lentis length	0.80 **	0.24 NS	0.34 NS
Lens thickness	0.82**	−0.34 NS	0.57*

Abbreviation: NS, not statistically significant ($p > .05$).
*There is a difference between means at $p < .05$ level.
**There is a difference between means at $p < .01$ level.

those reported in the literature (Tanimura, 1977; Taşbaş, 1985); however, no information is available in the literature regarding the bundle-shaped structures observed in brachycephalic dog breeds.

Some researchers have investigated the existence of a correlation between the morphometric values of the structures forming the eyeballs (Paunksnis et al., 2001; Williams, 2004). Paunksnis et al. (2001) have reported the correlations among lens thickness, vitreous body thickness, and the axis of the eyeball, and Williams (2004) has reported the correlations between lens thickness and the axis of the eyeball. According to our statistical findings, sex and age did not affect the number of ciliary processes; they varied according to the size of the skull structure. In addition, a non-significant negative correlation ($p > .05$) was observed between the lens thickness and the number of ciliary processes in brachycephalic dog breeds, whereas a positive correlation was determined for the same characteristics in mesocephalic dog breeds. A positive correlation was also found between the lens thickness and the number of dog breeds regardless of breed. The reason for the negative correlation between the aforementioned traits in

brachycephalic dog breeds is attributed to depression in the posterior surface of the lens of dogs with this skull structure.

Williams (2004) and Paunksnis et al. (2001) have reported lens thicknesses of 6.7 ± 1.0 mm and 4.7–6.8 mm, respectively, in dogs studied regardless of their breed. In the present study, the lens thickness was measured as 4.96 ± 0.02 mm in the brachycephalic dog breeds and 7.61 ± 0.13 mm in the mesocephalic dog breeds. Williams (2004) reported the lens thickness/eyeball diameter ratio as 0.33 (±0.1) mm. In the present study, the lens thickness (6.58 ± 0.24)/eyeball diameter ratio obtained without considering cranial structures was found to be 0.32 ± 0.1 mm, consistent with that reported in the literature (Williams, 2004). The fact that the posterior lens surface is more convex than the anterior lens surface in dogs with a mesocephalic skull structure is consistent with that reported in the literature (Murphy et al., 2013; Taşbaş, 1985). However, depression was observed in the facies posterior of the lens in dogs with a brachycephalic skull structure. This was considered an important difference, and no literature reporting the presence of depression in the posterior lens surface is available. Consistent with that reported in the literature (Murphy et al., 2013; Taşbaş, 1985), the lens capsule is very thin, the lens nucleus is located in the center, and the laminae lentis regularly progresses from the lens cortex to the center. Our observation of variable hook-shaped structures in the lens nucleus is consistent with that reported in the literature (Bassnett et al., 2011).

The findings that the ciliary zone, which is one of the parts forming the iris, is shaped thicker than the pupillary zone and that the depth of the plicae iridis is lesser and the width is greater corroborate those reported by Taşbaş (1985). The position of the angulus iridocorneal angle, the trabecular network structure in this region, and the presence of the pectinate ligament found in this study were compatible with those reported in the literature (Akbalık et al., 2015; Murphy et al., 2013; Simoens et al., 1996; Taşbaş, 1985).

AUTHOR CONTRIBUTIONS

Cengizhan Yılmaz: Writing – review and editing; methodology; writing – original draft; conceptualization; visualization. **Murat Kabak:** Writing – review and editing; methodology; data curation; writing – original draft. **Sedef Selviler Sizer:** Writing – review and editing; methodology; resources; writing – original draft.

CONFLICT OF INTEREST STATEMENT

The authors declare no conflicts of interest.

DATA AVAILABILITY STATEMENT

The data that support the findings of this study are available from the corresponding author upon reasonable request.

ORCID

Cengizhan Yılmaz https://orcid.org/0009-0007-3144-8907
Murat Kabak https://orcid.org/0000-0003-4255-1372
Sedef Selviler Sizer https://orcid.org/0000-0002-1990-4507

REFERENCES

Akbalık, M. E., Erdoğan, S., Sağsöz, H., & Saruhan, B. G. (2015). *A morphological study on iridocorneal angle and ciliary body of the Anatolian Shepherd Dogs (Canis familiaris)*. Kafkas Üniversitesi Veteriner Fakültesi Dergisi.

Akers, R. M., & Denbow, D. M. (2013). *Anatomy and physiology of domestic animals*. John Wiley & Sons.

Bacha, J., William, J., & Bacha, L. M. (2012). *Color atlas of veterinary histology*. John Wiley & Sons.

Bassnett, S., Shi, Y., & Vrensen, G. F. (2011). Biological glass: structural determinants of eye lens transparency. *Philosophical Transactions of the Royal Society B: Biological Sciences*, *366*(1568), 1250–1264.

Chiwitt, C. L., Baines, S. J., Mahoney, P., Tanner, A., Heinrich, C. L., Rhodes, M., & Featherstone, H. J. (2017). Ocular biometry by computed tomography in different dog breeds. *Veterinary Ophthalmology*, *20*(5), 411–419.

Diesem, C. (1975). In R. Getty (Ed.), *The anatomy of the domestic animals* (Vol. II, 5th ed.). W.B. Saunders Company.

Dyce, K. M., Sack, W. O., & Wensing, C. J. G. (2009). *Textbook of veterinary anatomy-E-Book*. Elsevier Health Sciences.

Easterling, R. (2015). *Fundamentals of Statistical Experimental Design and Analysis* (1st ed.). John Wiley & Sons.

Gaiddon, J., Rosolen, S., Steru, L., Cook, C., & Peiffer, R. (1991). Use of biometry and keratometry for determining optimal power for intraocular lens implants in dogs. *American Journal of Veterinary Research*, *52*(5), 781–783.

García-Sánchez, G. A., Gil-Carrasco, F., Román, J. J., Brooks, D. E., Álvarez-Clau, A., Hosgood, G., Iwabe, S., & Moreno-Mendoza, N. A. (2007). Measurement of retinal nerve fiber layer thickness in normal and glaucomatous Cocker Spaniels by scanning laser polarimetry. *Veterinary Ophthalmology*, *10*, 78–87.

Getty, R. (1965). *Anatomy of the dog* (Vol. 17). WB Saunders Company.

Gilger, B. C., Reeves, K. A., & Salmon, J. H. (2005). Ocular parameters related to drug delivery in the canine and equine eye: aqueous and vitreous humor volume and scleral surface area and thickness. *Veterinary Ophthalmology*, *8*(4), 265–269.

Gwin, R., Lerner, I., Warren, J., & Gum, G. (1982). Decrease in canine corneal endothelial cell density and increase in corneal thickness as functions of age. *Investigative Ophthalmology & Visual Science*, *22*(2), 267–271.

Kafarnik, C., Fritsche, J., & Reese, S. (2007). In vivo confocal microscopy in the normal corneas of cats, dogs and birds. *Veterinary Ophthalmology*, *10*(4), 222–230.

Kassab, A., & El-Zoghby, I. (2010). Anatomical and histological studies of the aqueous outflow system in the eye of goat (*Capra hircus*). *Journal of Veterinary Anatomy*, *3*(2), 13–22.

König, H. E., & Liebich, H.-G. (Eds.). (2020). *Veterinary anatomy of domestic animals: Textbook and colour atlas*. No Title.

Kreuzer, R., & Sivak, J. (1985). Chromatic aberration of the vertebrate lens. *Ophthalmic and Physiological Optics*, *5*(1), 33–41.

Leeson, C. R., Leeson, T. S., & Paparo, A. A. (1985). *Textbook of histology*. No Title.

Lynch, G. L., & Brinkis, J. L. (2006). The effect of elective phacofragmentation on central corneal thickness in the dog. *Veterinary Ophthalmology*, *9*(5), 303–310.

Mc Menamin, P. G., & Steptoe, R. J. (1991). Normal anatomy of the aqueous humour outflow system in the domestic pig eye. *Journal of Anatomy*, *178*, 65–77.

McGreevy, P., Grassi, T. D., & Harman, A. M. (2003). A strong correlation exists between the distribution of retinal ganglion cells and nose length in the dog. *Brain Behavior and Evolution*, *63*(1), 13–22.

Morishige, N., Wahlert, A. J., Kenney, M. C., Brown, D. J., Kawamoto, K., Chikama, T.-I., Nishida, T., & Jester, J. V. (2007). Second-harmonic imaging microscopy of normal human and keratoconus cornea. *Investigative Ophthalmology & Visual Science*, *48*(3), 1087–1094.

Murphy, C., Samuelson, D. A., & Pollock, R. V. H. (2013). In L. A. Evans (Ed.), *Miller's Anatomy of the Dog* (Vol. 21, 4th ed.). Elsevier Saunders.

Murphy, C. J., Zadnik, K., & Mannis, M. (1992). Myopia and refractive error in dogs. *Investigative Ophthalmology & Visual Science*, *33*(8), 2459–2463.

Mutti, D. O., Zadnik, K., & Murphy, C. J. (1999). Naturally occurring vitreous chamber-based myopia in the Labrador retriever. *Investigative Ophthalmology & Visual Science*, *40*(7), 1577–1584.

Patruno, M., Perazzi, A., Martinello, T., Blaseotto, A., Di Iorio, E., & Iacopetti, I. (2017). Morphological description of limbal epithelium: searching for stem cells crypts in the dog, cat, pig, cow, sheep and horse. *Veterinary Research Communications*, *41*, 169–173.

Paunksnis, A., Svaldeniene, E., Paunksniene, M., & Babrauskiene, V. (2001). Ultrasonographic evaluation of the eye parameters in dogs of different age. *Ultragarsas/Ultrasound*, *39*(2), 48–51.

Schiffer, S. P., Rantanen, N., Leary, G., & Bryan, G. (1982). Biometric study of the canine eye, using A-mode ultrasonography. *American Journal of Veterinary Research*, *43*(5), 826–830.

Simoens, P., De Geest, J.-P., & Lauwers, H. (1996). Comparative morphology of the pectinate ligaments of domestic mammals, as observed under the dissecting microscope and the scanning electron microscope. *Journal of Veterinary Medical Science*, *58*(10), 977–982.

Tanimura, I. (1977). Comparative morphology of the bulbus oculi of the domestic animals revealed by scanning electron microscopy (author's transl). *Nihon juigaku zasshi. The Japanese Journal of Veterinary Science*, *39*(6), 643–656.

Taşbaş, M. (1985). *Komperatif Veteriner Anatomi Aeshesiologia-Duyu Bilimi*. Ankara Üniversitesi Veteriner Fakültesi Yayınları.

Williams, D. (2004). Lens morphometry determined by B-mode ultrasonography of the normal and cataractous canine lens. *Veterinary Ophthalmology*, *7*, 91–95.

How to cite this article: Yılmaz, C., Kabak, M., & Selviler Sizer, S. (2024). Comparative macroanatomical and scanning electron microscopy study of the eyeball in brachycephalic and mesocephalic dog breeds. *Microscopy Research and Technique*, *87*(10), 2408–2417. https://doi.org/10.1002/jemt.24624